This is a repository copy of *Organic and Third Phase in HNO3/TBP/n-Dodecane System: No Reverse Micelles*.

White Rose Research Online URL for this paper:
http://eprints.whiterose.ac.uk/120285/

Version: Accepted Version

Article:

Ivanov, P, Mu, J, Leay, L et al. (4 more authors) (2017) Organic and Third Phase in HNO3/TBP/n-Dodecane System: No Reverse Micelles. Solvent Extraction and Ion Exchange, 35 (4). pp. 251-265. ISSN 0736-6299

https://doi.org/10.1080/07366299.2017.1336048

© 2017 Taylor & Francis Group, LLC. This is an Accepted Manuscript of an article published by Taylor & Francis in Solvent Extraction and Ion Exchange on 30 May 2017, available online: http://www.tandfonline.com/10.1080/07366299.2017.1336048. Uploaded in accordance with the publisher's self-archiving policy.

Reuse
Items deposited in White Rose Research Online are protected by copyright, with all rights reserved unless indicated otherwise. They may be downloaded and/or printed for private study, or other acts as permitted by national copyright laws. The publisher or other rights holders may allow further reproduction and re-use of the full text version. This is indicated by the licence information on the White Rose Research Online record for the item.

Takedown
If you consider content in White Rose Research Online to be in breach of UK law, please notify us by emailing eprints@whiterose.ac.uk including the URL of the record and the reason for the withdrawal request.

eprints@whiterose.ac.uk
https://eprints.whiterose.ac.uk/

THE ORGANIC AND THE THIRD PHASE IN THE SYSTEM HNO_3/TBP/n-DODECANE: NO REVERSE MICELLES

***P. Ivanov,[a] J. Mu,[b] L. Leay,[b,c] S.-Y. Chang,[b,d] C. A. Sharrad,[b,c] A. J. Masters,[b] S. L. M. Schroeder,[b,d,e]**

[a]National Physical Laboratory, Hampton Road, Middlesex, TW11 0LW Teddington, UK
[b]School of Chemical Engineering and Analytical Science, University of Manchester, M13 9PL, UK
[c]Research Centre for Radwaste and Decommissioning, Dalton Nuclear Institute, University of Manchester, M13 9PL, UK
[d](Present address) Diamond Light Source Ltd., Didcot, Oxfordshire, OX11 0DE, UK
[e](Present address) School of Chemical and Process Engineering, University of Leeds, Leeds LS2 9JT, UK

The composition and speciation of the organic and third phases in the system HNO_3/TBP/n-dodecane have been examined by a combination of gravimetry, Karl Fischer analysis, chemical analysis, FTIR and ^{31}P NMR spectroscopy, with particular emphasis on the transition from the two-phase to the three-phase region. Phase densities indicate that third phase formation takes place for initial aqueous HNO_3 concentrations above 15 M, whilst the results from the stoichiometric analysis imply that the organic and third phases are characterized by two distinct species, namely the mono-solvate $TBP \cdot HNO_3$ and the hemi-solvate $TBP \cdot 2HNO_3$, respectively. Furthermore, the ^{31}P-NMR spectra of organic and third phase show no significant chemical differences at the phosphorus centres, suggesting that the second HNO_3 molecule in the third phase is bound to HNO_3 rather than TBP. The third phase FTIR spectra reveal stronger vibrational absorption bands at 1028, 1310, 1653 and 3200-3500 cm^{-1}, reflecting higher concentrations of H_2O, HNO_3 and TBP. The molecular dynamics simulation data predict structures in accord with the spectroscopically identified speciation, indicating inequivalent HNO_3 molecules in the third phase. The predicted structures of the organic and third phases are more akin to microemulsion networks rather than the distinct, reverse micelles assumed in previous studies. H_2O appears to be present as a disordered hydrogen-bonded solvate stabilising the polar TBP/HNO_3 aggregates in the organic matrix, and not as a strongly bound hydrate species in aggregates with defined stoichiometry.

Keywords: Third phase formation, PUREX, solvent extraction, nitric acid, tributyl phosphate, molecular dynamics simulations

*Correspondence: peter.ivanov@npl.co.uk

INTRODUCTION

The principal method for reprocessing of spent nuclear fuel is the PUREX (Plutonium URanium EXtraction) process, which is based on solvent extraction of the two actinide elements from nitric acid solutions by tri-n-butyl phosphate (TBP), dissolved in either odourless kerosene or the aliphatic hydrocarbon n-dodecane.[1] Extraction systems built on such organophosphorus ligands dissolved in aliphatic solvents can suffer from third phase formation, when threshold concentrations of extracted metal and/or acid are exceeded. Such third phase formation is exhibited also by N-based extractants such as amides, as well as tetraalkylammonium salts and amines. [2-5] Third phase formation is readily recognisable as a separate, dense organic phase enriched in extractant, acid and metal relative to the lighter organic phase. Formation of third phase is an undesirable process in the reprocessing of spent fuel, as it could potentially cause safety and even criticality concerns due to the high metal concentrations and can lead to phase inversion issues. [6] Third phase formation is often considered to be the result of limited solubility of metal-ligand complexes in the organic medium, so that the colloidal suspension formed by TBP acting as a surfactant becomes favourable at higher metal loadings. [7, 8] The phase splitting process in a variety of TBP-based systems has for some time been considered to be associated with the formation of a microemulsion consisting of reverse micellar structures with a polar water core containing ionic species surrounded by a layer of extractant molecules.[9]

A number of studies have investigated the process of third phase formation in terms of phase boundaries, mainly studying the limiting organic concentration (LOC), defined as the threshold metal and acid concentrations in the organic phase at which phase splitting occurs. For a more sophisticated treatment of this phase behaviour, we refer to the research of Bauer et al.[10] Third phase formation in extraction of actinides by neutral organophosphorus extractants, including phase boundaries and factors affecting the process of phase splitting, has been thoroughly reviewed.[11] Investigation of the organic phase speciation of neptunium and plutonium in relation to the process of third phase formation has been conducted and the third phase boundaries have been reported.[12] The phenomenon of phase splitting during the extraction of plutonium with TBP in n-dodecane from nitric acid has been studied using small angle neutron scattering (SANS), which indicated that TBP in contact with aqueous phase containing nitric acid and plutonium forms small reverse micelles incorporating three to five TBP molecules. [6] The third-phase formation during the extraction of thorium nitrate from solutions with near-zero free acidity by 1.1M solutions of tri-n-butyl phosphate (TBP) and tri-n-amyl phosphate (TAP) in n-octane, n-decane, n-dodecane, n-tetradecane, and n-hexadecane have been studied and it was found the difference in solute concentrations and density between the third phase and the diluent-rich phase, as well as the ratio of the volume of diluent-rich phase to that of the third phase, can be treated as indices of the third-phase formation tendency.[13]

Some mineral acids cause third phase formation with TBP dissolved in aliphatic organic solvents even in the absence of metal ions. For example, the phase splitting phenomenon has been observed at very high nitric acid concentrations in the system HNO_3-TBP in cases when long-chain aliphatic solvents such as n-dodecane are used as TBP diluents.[9] Similarly, the extraction of sulfuric acid by tri-butyl phosphate-kerosene solutions results in three-phase formation at H_2SO_4 concentrations from 6.8 to 16 M, independent of the initial TBP concentration.[14] The tendency towards third phase formation of inorganic acids with 0.73 M TBP dissolved in n-octane in terms of decreasing LOC values was found to decrease in the order: $HClO_4 > H_2SO_4 > HCl > H_3PO_4 > HNO_3$.[15] This ordering has since been put on a quantitative basis. [2-4] A considerable amount of research has been devoted to its relationship with the Hofmeister series and we refer to references [11-13] for recent work in this area. Third phase formation in the system HCl/TBP/n-octane system was found to involve the simultaneous extraction of large amounts of water, bringing about organic phase splitting when the equilibrium HCl concentration in the aqueous phase becomes higher than 7.6 M. [19] The extraction by 1.1M tributyl phosphate in n-dodecane of perchloric and nitric acid was found to result in the formation of third phase in solutions with initial aqueous acidic concentration exceeding 2M $HClO_4$ or 15M HNO_3. [20] Based on small-angle X-ray (SAXS) and SANS evidence, the higher potential of perchloric acid for phase splitting the formation of third phase was attributed to the higher polarity of the perchlorate anion, which leads to more effective attractive interaction in the polar cores of the micellar structures. The phenomenon of phase splitting and formation of third phase occurs not only for TBP but across a range of neutral organo-phosphorous extractants when dissolved in long-chain non-polar, aliphatic solvents such as n-dodecane. Such extractants include TBPO, Octyl(Phenyl)-N,N-Diisobutyl Carbamoyl Methyl Phosphine Oxide (CMPO) and Dihexyl N,N-Diethyl Carbamoyl Methyl Phosphonate (DHDECMP). The third-phase formation tendency of DHDECMP varies across inorganic acids in the order $HClO_4 > HNO_3 > HCl > H_2SO_4$.[21] SANS studies suggest that the process of third-phase formation is driven by the formation of $DHDECMP{\cdot}HNO_3$ reverse micelles in the diluent phase. After phase separation the size of the aggregates in the third phase was found to be significantly smaller compared to those present when approaching the LOC, with the size of the entities in the heavy phase larger than in the light organic phase. [21]

The exact molecular structure and composition of the third phase entities remains unknown. In a recent study, simulation of the behaviour of TBP in the organic phase was carried out, with results suggesting that TBP self-assembles into a bi-continuous phase characterised by filamentous chains of TBP molecules formed by interaction of the oxygen and phosphorous moieties of adjacent TBP molecules. Formation of a molecular micro-emulsion structure was proposed, in which the filaments form a network.[22] The forcefield used in this study, however, overestimated the polarity of the TBP molecules [23] and simulation results using a higher quality forcefield are presented later in this article. Suffice it to state here that these later studies also revealed a micro-emulsion structure rather than reverse micelles. The process of organic phase splitting for several inorganic acids (HNO_3, $HClO_4$, H_2SO_4, and H_3PO_4) extracted with TBP in n-octane was investigated by SANS, which provided evidence for the existence of reverse micelles with diameters from 15 to 22 Å, with polar core diameters ranging from 10 to 15 Å.[24] For the extraction of HCl by TBP dissolved in n-octane the formation of reversed micelles with a maximum TBP aggregation number of 7 and a diameter of 19 Å has been reported.[24] An FTIR spectroscopy study of the system HNO_3/TBP/octane identified two structures, TBP·HNO_3 and TBP·2HNO_3.[25] The two nitric acid molecules in the hemi-solvate structure are spectroscopically inequivalent in the vibrations of the P=O bond, which led to the conclusion that the predominant structure of TBP·2HNO_3 involved hydrogen-bonded dimers of HNO_3, with only one of the HNO_3 molecules attached to TBP.[25]

In addition to the SANS and SAXS studies already mentioned, other studies with these techniques indicated the formation of large aggregates and reversed micelles in the heavy organic layer. [26-30] Specifically for the HNO_3-TBP system SAXS/SANS indicated that organic phases of TBP in equilibrium with acid solutions contains reverse micelles containing aggregates of 2 to 5 TBP molecules assembled around an aqueous polar core.[31]

The present gravimetric and spectroscopic study of the HNO_3/TBP/n-dodecane system was performed to examine third phase formation in this system more systematically and in more detail, particularly to generate additional information on the stoichiometry and the structure of the solvates in the third and organic phases. Shedding light on phase formation in the HNO_3/TBP/n-dodecane system is essential for better understanding more complex extraction systems, and is relevant to the industrial scale reprocessing of spent nuclear fuel.

EXPERIMENTAL

Materials

All reagents were analytical grade. Tri-n-butyl phosphate (Fisher Scientific, 99% purity, density 0.979 g ml^{-1}) was used as supplied without any further treatment. Anhydrous n-dodecane (99%, Sigma Aldrich) was used as a solvent for TBP solutions. Perchloric acid 70% (Merck) and 1 M NaOH in methanol (Fisher Scientific) were used for the determination of TBP and HNO_3 concentrations, respectively. All aqueous acidic solutions were prepared using 65% HNO_3 (Sigma Aldrich), 37% HCl

(Acros Organics) and 70% $HClO_4$ (Merck). Deionised water (18.2 MΩ·cm) was obtained using a Milli-Q water purification system.

Methods

Batch extraction experiments were carried out by mixing 5 ml of acidic solution containing HNO_3, HCl or $HClO_4$ at various concentration levels with an equal volume of 1.1 M (30% by volume) TBP dissolved in n-dodecane. Aqueous and organic samples were placed in 12 ml screw-cap polystyrene centrifuge tubes and intensively shaken for at least 10 min, then positioned upright for several hours to obtain equilibrium and allow phases to separate. As a next step, aliquots of the aqueous, organic and third phases were withdrawn with a 1000 µl Eppendorf pipette (max. error 0.35%) for further analysis. Mass densities were determined by measuring the weight of 1 ml aliquots on an Ohaus Galaxy 160D analytical balance with sensitivity of 10^{-4} g.

HNO_3 equilibrium concentrations in organic and third phase samples were determined by direct titration of aliquots with standardised 1 M NaOH solution in methanol using 1% phenolphthalein in ethanol as an indicator. The values reported below represent averages of three consecutive titration measurements. TBP equilibrium concentrations in third phase aliquots were determined volumetrically, determining the volume of the third phase formed by equilibrating the sample with an equal volume of 10 M $HClO_4$. The method requires calibration, conducted by measuring the exact volume of the third phase formed in a number of solutions with known TBP concentration, as described elsewhere.[29, 21] For samples that did not form a third phase, the concentration of TBP in the organic phase was considered to be equal to the initial one, based the negligible TBP solubility in aqueous media. Equilibrium water content in the organic and third phase samples was measured by coulometric titration method using a C20 Compact Karl Fischer coulometric titrator (Mettler-Toledo Inc.).

Infrared spectra of organic and third phase samples were recorded using a Nicolet iS10 FT-IR spectrometer (Thermo Scientific). The ^{31}P NMR spectroscopy of organic and third phase samples in 5 mm PTFE NMR tubes was performed using a B400 Bruker AVANCE III NMR spectrometer operating at 161.91 MHz. All spectroscopic measurements were carried out at room temperature.

Molecular Dynamics Simulations were performed for an organic phase and a third phase using the experimentally determined compositions shown in Table 1. Simulations were performed using the GROMACS package [32-34] at a pressure of 1 bar and a temperature of 298.15 K, using the Parrinello-Rahman barostat [35, 36] and Nosé-Hoover thermostat.[37, 38] The number of TBP, n-dodecane, HNO_3 and H_2O molecules were 278, 1267, 255 and 30 respectively for the organic phase, and were 597, 711, 1197 and 293 respectively for the third phase. The time step was 1 fs. The systems were equilibrated for 10 ns and the results quoted were averaged over runs of 10 ns. The force field used was the OPLS-2005 [39], where the partial charges on TBP were optimised. [23]

RESULTS AND DISCUSSION

Third phase boundaries

In order to study the concentration boundaries of the third phase formation, extraction experiments were conducted by equilibrating equal volumes of nitric acidic solutions with 1.1 M tri-n-butyl phosphate dissolved in n-dodecane. Mass densities of the aqueous and both organic phases were measured as a function of initial HNO_3 concentration, which was in the range between 1.1 and 15.8 M as shown in Fig. 1.

Figure 1. Density of aqueous, organic and third phase in the system HNO_3-1.1 M TBP / n-dodecane as a function of the initial HNO_3 concentration in the aqueous phase

From the results given in Fig. 1, it can be seen that the aqueous phase density depends linearly on the initial HNO_3 concentration and reaches a maximum value of 1.46 $g{\cdot}ml^{-1}$ for the sample containing 15.8 M initial HNO_3. A two phase region exists below initial HNO_3 concentration of 15 M. Beyond that point the organic phase splits forming a three phase region; 15 M initial HNO_3 appears to be the threshold value for phase splitting. In the two phase region, the organic phase density remains steady in the range between 0.85 and 0.90 $g{\cdot}ml^{-1}$. After the threshold concentration, a third phase is formed, causing a decrease in the organic phase density from 0.90 to 0.85 g·ml^{-1} while the third phase density increased from 0.90 to 1.0 g·ml^{-1}. The light organic phase after the splitting contains mainly diluent, while HNO_3 and TBP are concentrated in the heavy organic phase, which explains the differences in the phase densities. The limiting density of the aqueous phase corresponding to the phase splitting threshold is approximately 1.43 g·ml^{-1} or 15 M initial HNO_3 concentration. These values are significantly higher compared to the limiting aqueous density of the HNO_3 phase in case of 0.8 M DHDECMP in n-dodecane, which was found to be 1.03 g·ml^{-1}, corresponding to 1.1 M initial aqueous HNO_3 concentration.[21] This indicates that TBP is more resistant towards phase splitting and the formation of third phase compared to other neutral organophosphorous extractants such as DHDECMP.

Effect of different acids

In a separate series of measurements the occurrence of third phase in systems containing HCl, HNO_3 or $HClO_4$ mixed with TBP was studied and the phase densities were determined by mixing 5 ml of the acidic solution with an equal volume of 1.1 M TBP in n-dodecane. In order to investigate the effect of changing the mineral acids the differences between the densities of the heavy and light organic phases for these three systems were determined at initial acid concentrations immediately higher than the LOC (Fig. 2).

Figure 2. Equilibrium density of aqueous, organic and third phase for systems containing HCl, HNO_3 and $HClO_4$ with 1.1 M TBP in n-dodecane. The data for each system refer to an initial acid concentration immediately higher than that corresponding to the LOC.

The density difference between the light and heavy organic phases decreased in the following order: $HClO_4$/TBP > HCl/TBP > HNO_3/TBP. Density differences have previously been considered as an indicator for the tendency to form a third phase.[40] Therefore, based on the experimental results presented in Fig. 2, it can be concluded that $HClO_4$ has the strongest tendency to form third phase with TBP, followed by HCl and HNO_3. In line with this, a previous study concluded that the $HClO_4$ system is characterised by much stronger water transfer into the organic phase than for H_3PO_4 and HNO_3.[24] The potential for the formation of third phase during the extraction of inorganic acids by TBP appears to be associated with the acidity strength of the acids, with the pK_a values following the order $HClO_4$ > HCl > HNO_3. This suggests that a better ability to transfer protons may stabilise a more extensive water network solvating the acid in the organic matrix, and thus stabilising the third relative to the organic phase. Again we note the similarity of these results with those published for diamides and it is likely that the same molecular mechanisms are involved. [41] Furthermore, it has been reported that the acid strength order applies only to monoprotic acids. Chiarizia and Briand[15] have demonstrated that if one considers also H_2SO_4 and H_3PO_4, the pKa values do not follow the tendency to phase splitting, which indicates that third phase formation is a more complex phenomenon.

Equilibrium TBP, HNO_3 and H_2O concentrations

The equilibrium nitric acid concentrations in both organic and third phase samples with initial aqueous HNO_3 concentration ranging from 1.1 to 15.8 M and initial organic TBP concentration of 1.1 M were determined by direct titration of phase aliquots with standard NaOH solution in methanol. The results reveal an increase of the equilibrium HNO_3 levels in the organic phase (Fig. 3), from negligible up to 1.1 M as a function of the initial HNO_3 concentration. The equilibrium nitric acid, water and TBP concentrations, measured in the organic and third phases of systems with highest initial aqueous nitric acid loading of 15.8 M are summarised in Table 1.

Figure 3. Equilibrium HNO_3, TBP and H_2O concentrations in the organic and third phase vs. the initial aqueous HNO_3 concentration.

The equilibrium organic HNO_3 concentration sharply decreases when the third phase formation boundary is crossed (Fig. 3). It is noteworthy that within the two phase region the equilibrium HNO_3

concentration in the organic phase never exceeds the TBP concentration of 1.1 M in the organic phase. This value is exceeded in the third phase that appears at higher HNO_3 concentrations, in which a maximum value of 3.2 M is reached (Fig. 3).

A similar trend is evident for the equilibrium molar concentration of H_2O in the organic and third phase samples as determined by Karl Fischer titration (Table 1 and Fig. 3). It can be seen that the distribution of H_2O in the system HNO_3/TBP/n-dodecane mirrors the extraction behaviour of HNO_3, indicating that HNO_3 extraction is accompanied by water transfer from the aqueous to the organic phase. In the absence of third phase formation, the fraction of H_2O transferred to the organic phase is relatively small and increases steadily from 0.17 to 0.24 M as the initial HNO_3 concentration is increased. Once the LOC threshold value is exceeded the majority of the organic phase H_2O molecules are transferred to the third phase, as evident through a decrease of the H_2O content in the organic phase by approximately an order of magnitude.

Taking into account that TBP solubility is negligible in the aqueous phase, the equilibrium concentration of TBP in the organic phase of the two-phase systems can be assumed to be equal to the initial TBP concentration. For the three-phase systems, the concentration of TBP in the light organic phase was determined by measuring the volume of the heavy organic phase produced by equilibrating of 5 ml aliquot of the organic phase with an equal volume of 10 M $HClO_4$, as described in the Experimental section. Results indicate that TBP is significantly more concentrated in the third phase compared to the light organic phase. In summary, our compositional analysis indicates that the third phase is enriched in H_2O, HNO_3 and TBP relative to the organic phase, which is depleted in these compounds and mainly contains solvent.

Table 1. Equilibrium concentrations of H_2O, HNO_3 and TBP in the organic and third phases with initial aqueous HNO_3 concentration of 15.8 M

Based on the stoichiometric data given in Table 1, the equilibrium concentration of TBP in the organic phase appears to be approximately equal to the sum of nitric acid and water equilibrium concentrations:

$$[\mathrm{TBP}]_{\mathrm{org}} = [\mathrm{HNO_3}]_{\mathrm{org}} + [\mathrm{H_2O}]_{\mathrm{org}}$$

The water concentration is a fraction (approximately 12%) of the HNO_3 concentration. This suggests that the main species in the organic phase is the mono-solvate $TBP{\cdot}HNO_3$, perhaps accompanied by monohydrate $TBP{\cdot}H_2O$ or the ternary species $TBP{\cdot}HNO_3{\cdot}H_2O$.

The equilibrium concentration of HNO_3 in the third phase was twice higher than the equilibrium TBP concentration:

$$[\mathrm{HNO_3}]_{\mathrm{3rd}} = 2[\mathrm{TBP}]_{\mathrm{3rd}}$$

This stoichiometric ratio suggests that the predominant species in the third phase is the hemi-solvate $TBP{\cdot}2HNO_3$. Adding a second HNO_3 molecule to the mono-solvate $TBP{\cdot}HNO_3$ would increase the polar character of the assemblies, thus decreasing solubility of the species in neutral organic solvent and facilitating the formation of the third phase, in which a higher concentration of water can stabilise

^{31}P NMR spectroscopy

Two structurally different models for the third phase $TBP{\cdot}2HNO_3$ hemi-solvates have been suggested in the literature with the main being the exact location where the second HNO_3 molecule is bound to the existing $HNO_3{\cdot}TBP$ mono-solvate molecule. The second HNO_3 molecule could be directly attached to the P=O group of the tributyl phosphate forming a parallel HNO_3 structure.[42] Other studies indicated that the second HNO_3 molecule is linked to the solvate by a hydrogen bond between the two HNO_3 molecules, forming a chain $TBP{\cdot}HNO_3{\cdot}HNO_3$ structure.[25] In an attempt to shed additional light on this issue and to determine the structures of $TBP{\cdot}HNO_3$ solvates, a ^{31}P-NMR characterisation of both organic and third phase samples was performed (Fig. 4).

Figure 4. ^{31}P-NMR spectra of organic (left) and third phase samples (right) of 16 M HNO_3-1.1 M TBP/n-dodecane system

The formation of chemical and hydrogen bonds as well as rearrangements and modifications of the partial chemical structure around the phosphorus centres could lead to changes in the electron density and hence in chemical shifts in the ^{31}P-NMR spectrum. [43] Attaching a second HNO_3 molecule directly to the TBP phosphate group should result in a downfield ^{31}P chemical shift relative to the organic phase mono-solvate. However, experimental organic and third phase ^{31}P-NMR spectra (Fig. 4) reveal no strong difference, as both spectra consist of a single narrow signal with chemical shifts of -1.64 and -1.54 ppm, respectively. The relatively narrow peak widths of less than 10 ppm suggest that the composition of TBP species is rather uniform, with no distribution of chemically distinct species.[44]

Fig. 5. Proposed structure of the third phase $TBP{\cdot}2HNO_3$ hemi-solvates

The lack of significant chemical shift in the third phase ^{31}P-NMR spectrum compared to the spectrum of the organic phase provides a strong indication that the third phase formation and the addition of an extra HNO_3 molecule to the organic $TBP{\cdot}HNO_3$ mono-solvates is not associated with the immediate chemical surroundings of phosphorus moieties in TBP. Therefore, it appears likely that the third phase solvate structure involves two HNO_3 molecules hydrogen-bonded to each other forming a chain $TBP{\cdot}HNO_3{\cdot}HNO_3$ structure as shown in Fig. 5.

Figure 6. IR spectra of organic phase samples with initial aqueous HNO_3 concentration of 2, 4, 6, 8, 10, 12 and 14 M (from bottom to top)

Infrared spectroscopy

Organic samples with various initial aqueous HNO_3 concentrations were also analysed using infrared spectroscopy (Figure 6). There is a sharp increase in the intensity of the peaks at 1653 and 1310 cm^{-1} with increasing initial aqueous HNO_3 concentration. These peaks stem from the asymmetric NOO stretching (1700-1620 cm^{-1}) and the symmetric NOO stretching (1330-1280 cm^{-1}).[25, 43] The increase in the intensities of these bands with an increase in aqueous HNO_3 concentration despite the decrease in HNO_3 concentration quantified (figure 3) is due to the increase in mono-solvate $TBP{\cdot}HNO_3$ concentration in the organic phase. The broad peak at 3500-3200 cm^{-1} also increased in intensity which corresponds to the O-H stretching band of HNO_3, in line with the higher HNO_3 concentrations in the organic phase (see fig. 3) as a function of aqueous HNO_3 concentration. The intensity of the vibrational bands at 1028 cm^{-1} (P-O-C stretch),[28] related to the TBP concentration together with the triplet at 3000-2800 cm^{-1} (C-H stretch), showed no significant differences indicating that the equilibrium concentrations of TBP and n-dodecane remain constant.

Table 2. Major vibrational bands relevant to the HNO_3-TBP system [25]

The infrared spectra of both organic and third phases with an initial aqueous HNO_3 concentration of 15.1 M were also measured (Fig. 7). Both spectra include identical sets of vibrational bands. The main differences between the organic and third phase IR spectra are in the intensities of some vibrational bands. The third phase spectrum shows higher peak intensities at 1028, 1310, 1653 and 3200-3500 cm^{-1} compared to the organic phase. These higher intensities are in line with the higher concentrations of H_2O, HNO_3 and TBP in the third phase. The intensity of the 3000–2850 cm^{-1} band (C-H stretch) decreases in the third phase spectra, reflecting the fact that the n-dodecane concentration is lower than in the organic phase.

Figure 7. IR spectra of organic vs. third phase samples with initial aqueous HNO_3 concentration of 15.1 M

Molecular Dynamics Simulations

In order to obtain structure models for the organic and third phases molecular dynamics simulations[45] were performed for an organic phase and a third phase using the experimentally determined compositions shown in Table 1. Simulation snapshots of the two phases, where for clarity only 2 nm slices are shown, are shown in Figures 8 and 9. While the structures shown are mobile and will flex and bend, the basic topology does not alter with time. We see no evidence of reverse micelles. Instead the structure resembles a bi-continuous emulsion on the molecular scale, with the TBP molecules acting as surfactants. The butyl groups of the TBP are in contact with the dodecane diluent, while polar molecules, such as nitric acid and water, are associated with the polar phosphate groups.

Figure 8. A snapshot of the organic phase system. TBP, HNO_3 and H_2O molecules are represented in yellow, red and blue, respectively; n-dodecane molecules are not shown for clarity

If we consider the organic phase with a relatively low nitric acid concentration, we observed predominantly monodentate TBP-HNO_3 complexes. At higher nitric acid concentrations, corresponding to the observed third phase composition, we see TBP-HNO_3-HNO_3 complexes, in agreement with the conclusion drawn above from the ^{31}P NMR data. The water molecules are somewhat randomly distributed around the system and while one can occasionally find TBP-HNO_3-HNO_3-H_2O-HNO_3-HNO_3-TBP chains, they are not common. Our belief is that the experimentally observed stoichiometry does not stem from a significant presence of such extended structures.

Figure 9. A snapshot of the third phase system. TBP, HNO_3 and H_2O molecules are represented in yellow, red and blue, respectively; n-dodecane molecules are not shown for clarity

In addition, the average number of hydrogen bonds between molecule pairs was analysed. The criterion for determining the presence of a hydrogen bond was that the donor-acceptor distance should be no more than 0.35 nm and the acceptor-donor-hydrogen angle should be no more than 30°. The oxygen atoms that have covalent bonds with the hydrogen atoms in the H_2O and HNO_3 molecules were regarded as potential donors and the electronegative atoms that possess a lone electron pair were regarded as potential acceptors. The average numbers of hydrogen bonds between pairs of TBP, HNO_3 or H_2O molecules are shown in Table 3.

Table 3. Average numbers of hydrogen bonds between molecule pairs

To recap, the numbers of TBP, n-dodecane, HNO_3 and H_2O molecules used in the MD simulations were 278, 1267, 255 and 30 respectively for the organic phase, and 597, 711, 1197 and 293 respectively for the third phase.

In the light organic phase, the number of $TBP \cdot HNO_3$ hydrogen bonds is 231 (Table 3), which accounts for 91% of HNO_3 and 83% of TBP molecules. The number of $TBP \cdot H_2O$ hydrogen bonds is 33, which accounts for 111% of H_2O and 12% of TBP molecules. Note the 111% here indicates that 100% of H_2O molecules are connected with TBP and 11% of these are connected with two TBP molecules. The number of $HNO_3 \cdot HNO_3$ hydrogen bonds is only 4. These results indicate that there are large numbers of $TBP \cdot HNO_3$ dimers and only a small number of HNO_3-HNO_3 dimers. Hence $TBP \cdot HNO_3$ is the predominant structure in the light organic phase, in line with the experimental results. In addition, it is very likely that each H_2O molecule forms at least one hydrogen bond with a TBP molecule in the light organic phase.

In the third phase, however, the number of $TBP \cdot HNO_3$ hydrogen bonds is 619, which corresponds to 52% of HNO_3 and 104% of TBP molecules. Note the 104% here indicates that 100% of TBP molecules are connected with HNO_3 and 4% of these are likely bidentate species linked to two monodentate HNO_3 molecules. The number of HNO_3-HNO_3 hydrogen bonds is 284, which involves 47% of the HNO_3. The number of TBP-H_2O hydrogen bonds only accounts for 31% of H_2O, which is noticeably lower than in the light organic phase. These results could be explained by the formation of bidentate TBP·2HNO_3 complexes in the third phase, predominantly TBP-HNO_3-HNO_3 aggregates, again in line with the ^{31}P NMR results. In addition, the number of HNO_3-H_2O hydrogen bonds is almost twice the number of H_2O molecules, which indicates that one H_2O is typically shared between two HNO_3 molecules. Hence, HNO_3-H_2O-HNO_3 aggregates may be a common structure in the third phase. A very recent paper [46] also presents the results of molecular dynamics simulations of this system and the hydrogen bonding analysis is broadly in agreement with that given above.

Overall, the observed behaviour of the TPB/HNO_3/H_2O/dodecane system has much in common with oil/water/surfactant systems. The phases we report have similarities with the Winsor-III classification of surfactant micro-emulsion systems [47], where bi-continuous micro-emulsion phases are found. What differentiates our system from most surfactant systems, however, is that we believe we have phase co-existence between two bi-continuous micro-emulsion phases, both of isotropic symmetry. Most Winsor III phase diagram show, instead, co-existence between a bi-continuous and a micellar phase (or a phase of different symmetry). A recent review of surfactant phase behaviour is given by Hyde et al [48] and we note the work of Erlinger [5], which describes the transition of reverse micelles to a bi-continuous structure. It is interesting to note in this context the two level-cut Gaussian random wave representations of the micro-structure of bi-continuous structures [49,50], which show a striking resemblance to the molecular dynamics snapshots shown in Figures 8 and 9. The fact that the majority of water-poor microemulsion systems exhibit bicontinuous structures rather than reverse micelles gives, arguably, extra credence to the results we have presented.

CONCLUSIONS

Third phase boundaries of the system the system HNO_3-1.1 M TBP/n-dodecane were determined by measuring the phase densities. The formation of third phase occurred when the initial aqueous nitric acid concentration is higher than 15 M. Based on stoichiometric ratio analysis, two different species have been identified in the organic and third phase, mono-solvate TBP·HNO_3 and the hemi-solvate TBP·2HNO_3, respectively. The ^{31}P-NMR spectra of both organic and third phase have been obtained and no significant differences have been observed, suggesting that the attachment of a second HNO_3

molecule to the TBP·HNO_3 mono-solvate does not affect the chemical state of the phosphorus centres. This indicates that the TBP·2HNO_3 solvate structure involves two HNO_3 molecules, linked together in a chain of HNO_3 dimers in the form of TBP·HNO_3·HNO_3. Infrared spectra of the organic phase show that an increase in the intensity of the vibrational bands, assigned to O-H (3200-3500 cm^{-1}), asymmetric NOO (1620-1700 cm^{-1}) and symmetric NOO stretches (1280-1330 cm^{-1}) with increasing initial aqueous nitric acid concentration. The intensity of the vibrational bands associated with C-H stretch (2800-3000 cm^{-1}) and P-O-C stretch (1028 cm^{-1}) remain constant. Compared with the organic phase with identical initial aqueous HNO_3 concentration, the third phase spectrum shows stronger absorption at 1028, 1310, 1653 and 3200-3500 cm^{-1}, reflecting the fact that the third phase is enriched in H_2O, HNO_3 and TBP. Molecular dynamics simulation predict structures in accord with the experimentally observed spectroscopic data, indicating inequivalent HNO_3 molecules in the third phase. The structures of the organic and third phases are more akin to micro-emulsion networks than distinct, reverse micelles. Similarities with bi-continuous micro-emulsion phases in the Winsor-III classification of surfactant micro-emulsion systems are evident, although the current system appears to be characterised by phase co-existence between two isotropic bi-continuous micro-emulsion phases. The results of our molecular dynamics analysis of the microstructure are in line with previous Gaussian random wave representations of the micro-structure of bi-continuous structures. [49,50]

Acknowledgements. All data supporting this study are provided either in the results section of this paper or in the supplementary information accompanying it. We thank EPSRC for financial support under grant EP/I002855/1. The authors also thank to Dr. Stephanie Cornet for assistance with the NMR measurements. Sin-Yuen Chang thanks The University of Manchester as well as Mr and Mrs Clews for the Robert Clews Presidential PhD scholarship.

REFERENCES

1. Spent Fuel Reprocessing Options, IAEA-Tecdoc-1587, 2008.
2. Dejugnat, C., Berthon, L., Dubois, V., Dourdain, S., Meridiano, Y., Guillaumont, D., Pellet-Rostaing, S., Zemb, T. Liquid-liquid extraction of acids and water by a malonamide: I-Anion

specific effects on the polar core microstructure of the aggregated malonamide. Solvent Extr. Ion Exch. 2014, 32, 601-619.

3. Dourdain, S., Dejugnat, C., Berthon, L., Dubois, V., Pellet-Rostaing, S., Dufreche, J.F., Zemb, T. Liquid-liquid extraction of acids by a malonamide: II-anion specific effects in the aggregate –enhanced extraction isotherms. Solvent Extr. Ion Exch. 2014, 32, 620-636.
4. Dejugnat, C., Dourdain, S., Berthon, L., Dubois, V., Berthon, L., Pellet-Rostaing, S., Dufreche, J.F., Zemb, T. Reverse aggregate nucleation induced by acids in liquid-liquid extraction process. Phys. Chem. Chem. Phys. 2014, 16, 7339-7349.
5. Erlinger, C., Belloni, L., Zemb, T., Madic, C. Attractive interactions between reverse aggregates and phase separation in concentrated malonamide extractant solutions. Langmuir 1999, 15(7), 2290–2300.
6. Plaue, J.; Gelis, A.; Czerwinski, K. Plutonium third phase formation in the 30% TBP/nitric acid/hydrogenated polypropylene tetramer system. Solvent Extr. Ion Exch. **2006**, 24, 271-282.
7. Chiarizia, R.; Jensen, M.P.; Borkowski, M.; Ferraro, J.R.; Thiyagarajan, P.; Littrell, K.C. Third phase formation revisited: The U(VI), HNO_3–TBP, n-dodecane system. Solvent Extr. Ion Exch. **2003**, 21(1), 1-27.
8. Marcus, Y.; Kertes, A.S. Ion Exchange and Solvent Extraction of Metal Complexes; Wiley Interscience: New York, 1969; p. 715.
9. Osseo-Asare, K. Aggregation, reversed micelles and microemulsions in liquid-liquid extraction: The tri-n-butylphosphate- diluent- water- electrolyte system. Adv. Colloid Interface Sci. **1991**, 37, 123–173.
10. Bauer, C., Baudiun, P., Dufreche, J.F., Zemb, T., Diat, O. Liquid/liquid metal extraction: Phase diagram topology resulting from molecular interactions between extractant, ion, oil and water. Eur. Phys. J. Special Topics **2012**, 213, 225-241.
11. Vasudeva Rao, P.R.; Kolarik, Z. A review of third phase formation in extraction of actinides by neutral organophosphorus extractants. Solvent Extr. Ion Exch. **1996**, 14(6), 955-993.
12. Plaue, J.; Gelis, A.; Czerwinski, K. Actinide third phase formation in the 1.1M TBP/nitric acid/alkane diluent system. Solvent Extr. Ion Exch. **2006**, 41, 2065-2074.

13. Mallick, S.; Suresh, A.; Srinivasan T.G.; Vasudeva Rao, P.R. Comparative Studies on Third-Phase Formation in the Extraction of Thorium Nitrate by Tri-n-Butyl Phosphate and Tri-n-Amyl Phosphate in Straight Chain Alkane Diluents. Solvent Extr. Ion Exch. **2010**, 28, 459-481.
14. Fu, X.; Hu, X.P.; Zhang, Z.; Hu, Z.; Wang, D. Three phase extraction study. I. Tri-butyl phosphate-kerosene:H_2SO_4-H_2O extraction system. Colloid Surface A, **1999**, 152, 335-343
15. Chiarizia, R.; Briand, A. Third phase formation in the extraction of inorganic acids by TBP in n-octane. Solvent Extr. Ion Exch. **2006**, 24(3), 283-297.
16. Leontidis, E. Christoforou, M, Georgiou, C., Delclos, T. The ion-lipid battle for hydratation water and interfacial sites at soft-matter interfaces. Curr. Opinion Coll. Interf. Sci. **2014**, 19, 2-8.
17. Leontidis, E. Chaotropic salts interacting with soft matter: Beyond the lyotropic series. Curr. Opinion Coll. Interf. Sci. **2016**, 23, 100-109.
18. Schwierz, N., Horinek, D., Sivan, U., Netz, R.R. Reversed Hofmeister series- The rule rather than exception. Curr. Opinion Coll. Interf. Sci. **2016**, 23, 10-18.
19. Chiarizia, R.; Rickert, P.G.; Stepinski, D.; Thiyagarajan, P.; Littrell, K.C. SANS study of third phase formation in the HCl-TBP-n-octane system. Solvent Extr. Ion Exch. **2006**, 24(2), 125-148.
20. Nave, S.; Mandin, C.; Martinet, L.; Berthon, L.; Testard, F.; Madic C.; Zemb Th. Supramolecular organisation of tri-n-butyl phosphate in organic diluent on approaching third phase transition. Phys. Chem. Chem. Phys. 2004, 6, 799-808.
21. Lohithakshan, K.V.; Aswal, V.K., Aggarwal, S.K. Studies on the third phase formation in DHDECMP/dodecane/HNO_3. Radiochim. Acta **2011**, 99, 179-186.
22. Leay, L., Tucker, K., Del Regno, A., Schroeder, S.L.M., Sharrad, C.A., Masters, A.J. The behaviour of tributyl phosphate in an organic diluent. Mol. Phys. **2014**, 112(17), 2203-2214.
23. Mu, J., Motokawa. R., Williams. C.D., Akutsu. K., Masters. A.J., A Comparative Molecular Dynamics Study on Tri-n-butyl Phosphate in Organic and Aqueous Environments and its Relevance to Nuclear Extraction Processes. J. Phys. Chem. B, **2016**, 120 (23), 5183-5193.

24. Chiarizia, R.; Briand, A.; Jensen, M.P., Thiyagarajan, P. SANS study of reverse micelles formed upon the extraction of inorganic acids by TBP in n-octane. Solvent Extr. Ion Exch. **2008**, 26(4), 333-359.
25. Ferraro, J.R.; Borkowski, M.; Chiarizia, R.; McAlister, D.R. FT-IR spectroscopy of nitric acid in TBP/octane solution. Solvent Extr. Ion Exch. **2001**, 19(6), 981-992.
26. Chiarizia, R.; Jensen, M.P.; Borkowski, M.; Ferraro, J.R.; Thiyagarajan, P.; Littrell, K.C. SANS study of third phase formation in the U(VI)-HNO_3/TBP-n-dodecane system. Sep. Sci. Technol. **2003**, 38(12), 3313-3331.
27. Borkowski, M.; Chiarizia, R.; Jensen, M.P.; Ferraro, J.R.; Thiyagarajan, P.; Littrell, K.C. SANS study of third phase formation in the Th(IV)-HNO_3/TBP-n-octane system. Sep. Sci. Technol. **2003**, 38(12), 3333-3351.
28. Chiarizia, R.; Nash, K. L.; Jensen, M. P.; Thiyagarajan, P.; Littrell, K. C. Application of the Baxter Model for hard-spheres with surface adhesion to sans data for the U(VI)-HNO_3, TBP-n-dodecane system. Langmuir, **2003**, 19, 9592-9599.
29. Chiarizia, R.; Jensen, M. P.; Rickert, P. G.; Kolarik, Z.; Borkowski, M.; Thiyagarajan, P. Extraction of zirconium nitrate by TBP in n-octane: Influence of cation type on third phase formation according to the ‘‘sticky spheres’’ model. Langmuir, **2004**, 20, 10798-10808.
30. Plaue, J.; Gelis, A.; Czerwinski, K.; Thiyagarajan, P.; Chiarizia, R. Small-angle neutron scattering study of plutonium third phase formation in 30% TBP/HNO_3/alkane diluent systems. Solvent Extr. Ion Exch. **2007**, 25(3), 351-371.
31. Shilin, I. V.; Indikov, E. M.; Zhdanov, Yu. F.; Makarov, D. G. Method for determination of TBP in TBP- kerosene mixtures. USSR Patent 114,186, 1958.
32. Bekker, H., et al, Gromacs: A parallel computer for molecular dynamics simulations. Physics Computing. **1993**, 92, 252-256.
33. Berendsen, H.J., D. van der Spoel, and R. van Drunen, GROMACS: A message-passing parallel molecular dynamics implementation. Comput. Phys. Commun.. **1995**, 91, 43-56.
34. Van Der Spoel, D., et al., GROMACS: fast, flexible, and free. J. Comput. Chem. **2005**, 26, 1701-1718.

35. Parrinello, M. and A. Rahman, Polymorphic transitions in single crystals: A new molecular dynamics method. J. Appl. Phys. **1981**, 52, 7182-7190.
36. Nosé, S. and M.L. Klein, Constant pressure molecular dynamics for molecular systems. Mol. Phys. **1983**, 50, 1055-1076.
37. Nosé, S., A unified formulation of the constant temperature molecular dynamics methods. J. Chem. Phys. **1984**, 81, 511-519.
38. Hoover, W.G., Canonical dynamics: equilibrium phase-space distributions. Phys. Rev. A. **1985**, 31, 1695.
39. Banks, J.e.a., Integrated modeling program, applied chemical theory (IMPACT). J. Comput. Chem. **2005**, 26, 1752-1780.
40. Stoyanov, E.S., Mihailov, V.A., Chekmarev, A.M., Chizhevskaya, S.V. The composition and structure of the associates of nitric acid extracted from its concentrated aqueous solutions by 100% TBP. Russ. J. Inorg. Chem. **1990**, 35, 821-826.
41. Qiao, B., Ferru, G., De la Cruz, M.O., Ellis, R.J. Molecular origins of mesoscale ordering in a metalloamphiphile phase. ASC Cent. Sci. **2015**, 1, 493-503.
42. Uetake, N. Chemical state detection of dibutyl phosphate using ^{31}P NMR chemical shift change. Can. J. Chem. **1991**, 69, 322-326.
43. Sarsfield, M.J., Taylor, R.J., Maher, C.J. Neptunium(V) disproportionation and cation-cation interactions in TBP/kerosene solvent. Radiochim. Acta **2007**, 95, 677-682.
44. Urtake, N. Precipitation formation of zirconium dibutyl phosphate complex in Purex process. J. Nucl Sci. Technol. **1989**, 26(3), 329-338.
45. Rapaport, D.C., The art of molecular dynamics simulation. 2004: Cambridge university press.
46. Servis, M.J., Wu, D.T., Braley, J. Network analysis and percolation transition in gen bonded clusters: Nitric acid and water extraction by tributyl phosphate. Phys. Chem. Chem. Phys. 2017, DOI: 10.1039/C7CP01845B.
47. Winsor, P.A. Hydrotropy, solubilisation and related emulsification processes. Trans Faraday Soc., **1948**, 44, 376–398.
48. Hyde, S.H. et al. 1997. Colloids and Surfaces A, 129-130, 435-454.

49. Duvail, M., Dufreche, J.F., Arleth, L., Zemb, T. Mesoscopic modelling of frustration in microemulsions. Phys. Chem. Chem. Phys. **2013**, 15, 7133-7141.
50. Teubner, M. Level surfaces of Gaussian random fields and microemulsions. Europhys. Lett. **1991**, 14(5), 403-408.

CAPTIONS

Table 1. Equilibrium concentrations of H_2O, HNO_3 and TBP in the organic and third phases with initial aqueous HNO_3 concentration of 15.8 M

Table 2. Major vibrational bands relevant to the HNO_3-TBP system

Table 3. Average numbers of hydrogen bonds between molecule pairs

Figure 1. Density of aqueous, organic and third phase in the system HNO_3-1.1 M TBP / n-dodecane as a function of the initial aqueous HNO_3 concentration

Figure 2. Equilibrium density of aqueous, organic and third phase for systems containing HCl, HNO_3 and $HClO_4$ with 1.1 M TBP in n-dodecane. The data for each system refer to an initial acid concentration immediately higher than that corresponding to the LOC.

Figure 3. Equilibrium HNO_3, TBP and H_2O concentrations in the organic and third phase vs. the initial aqueous HNO_3 concentration

Figure 4. ^{31}P-NMR spectra of organic (left) and third phase samples (right) of 16 M HNO_3-1.1 M TBP/n-dodecane system

Figure 5. Suggested structure of the third phase TBP·$2HNO_3$ hemi-solvates

Figure 6. IR spectra of organic phase samples with initial aqueous HNO_3 concentration of 2, 4, 6, 8, 10, 12 and 14 M (from bottom to top)

Figure 7. IR spectra of organic vs. third phase samples with initial aqueous HNO_3 concentration of 15.1 M

Figure 8. The snapshot of the organic phase system. TBP, HNO_3 and H_2O molecules are represented in yellow, red and blue, respectively; n-dodecane molecules are not shown for clarity

Figure 9. The snapshot of the third phase system. TBP, HNO_3 and H_2O molecules are represented in yellow, red and blue, respectively; n-dodecane molecules are not shown for clarity

FIGURES AND TABLES

Table 1. Equilibrium concentrations of H_2O, HNO_3 and TBP in the organic and third phases with initial aqueous HNO_3 concentration of 15.8 M

Compound	Concentration in the organic phase, M	Concentration in the third phase, M
H_2O	0.08	0.77
HNO_3	0.68	3.15
TBP	0.74	1.57

Table 2. Major vibrational bands relevant to the HNO_3-TBP system [25]

Assignment	Frequency, cm^{-1}
P-O-C stretch	1028
P=O stretch	1282
NOO symmetric stretch	1304
NOO asymmetric stretch	1627

Table 3. Average numbers of hydrogen bonds between molecule pairs

Molecule pair	The light organic phase	The third phase
TBP – HNO_3	231	619
TBP – H_2O	33	89
HNO_3 – HNO_3	4	284
HNO_3 – H_2O	28	584
H_2O – H_2O	4	20

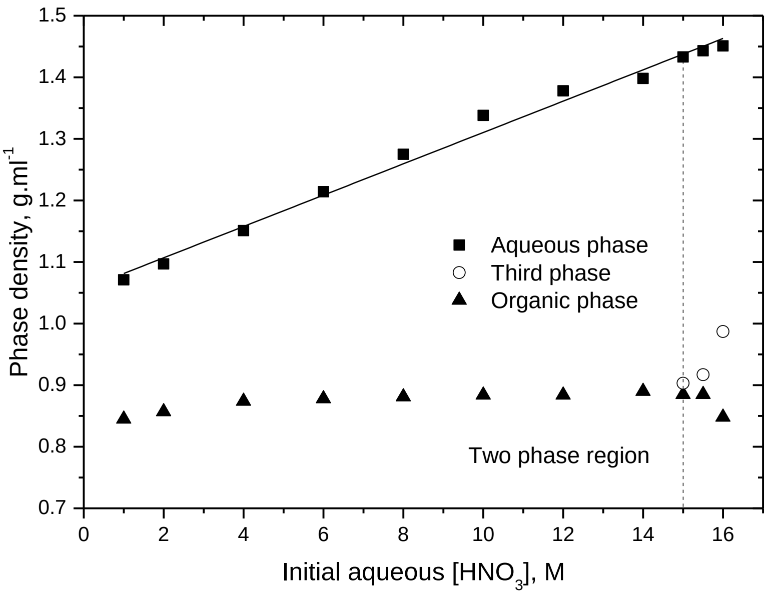

Figure 1. Density of the aqueous, organic and third phases in the system: HNO_3-1.1 M TBP / n-dodecane as a function of the initial HNO_3 concentration in the aqueous phase

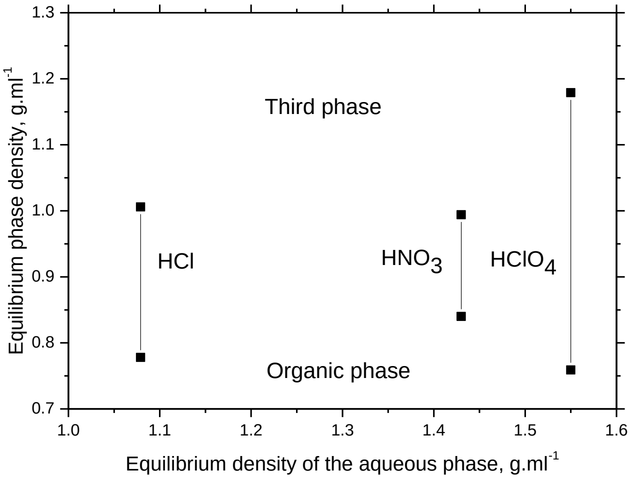

Figure 2. Equilibrium density of aqueous, organic and third phase for systems containing HCl, HNO_3 and $HClO_4$ with 1.1 M TBP in n-dodecane. The data for each system refer to an initial acid concentration immediately higher than that corresponding to the LOC.

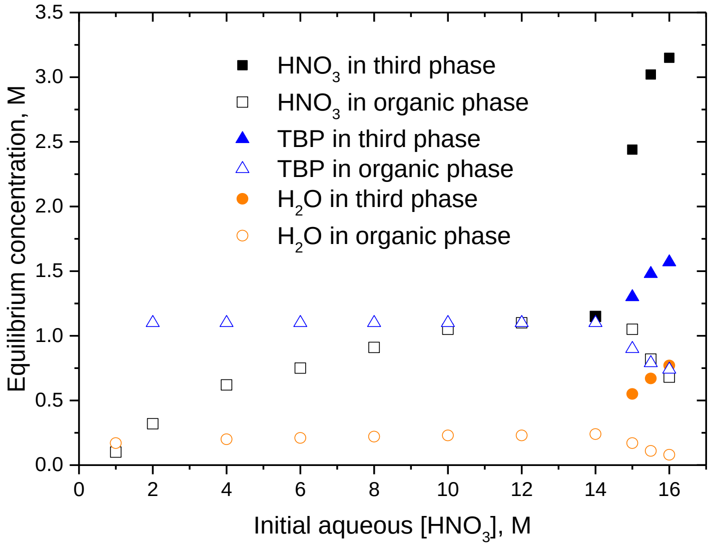

Figure 3. Equilibrium HNO_3, TBP and H_2O concentrations in the organic and third phase vs. the initial aqueous HNO_3 concentration

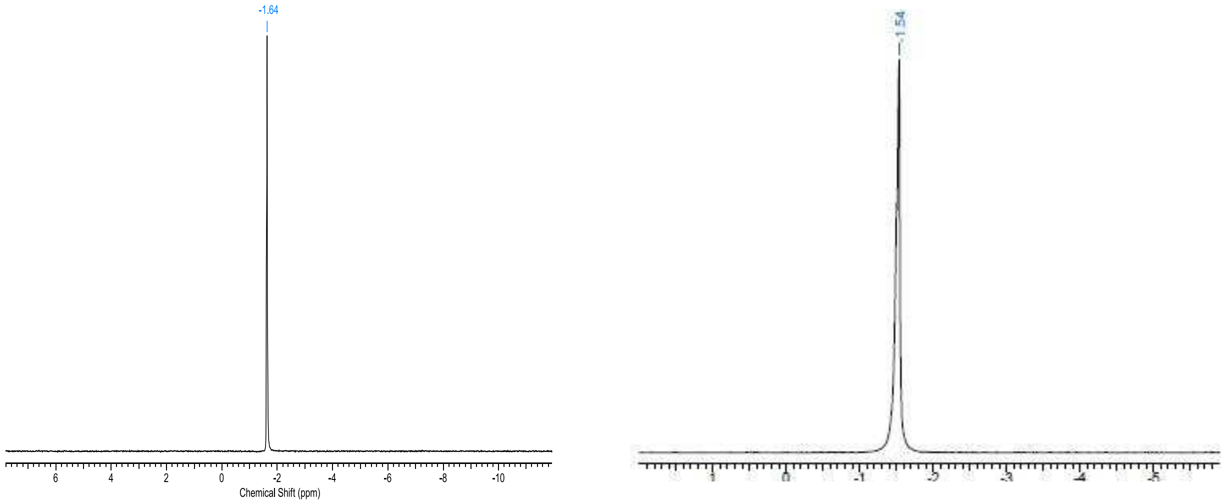

Figure 4. ^{31}P-NMR spectra of organic (left) and third phase samples (right) of 16 M HNO_3-1.1 M TBP/n-dodecane system

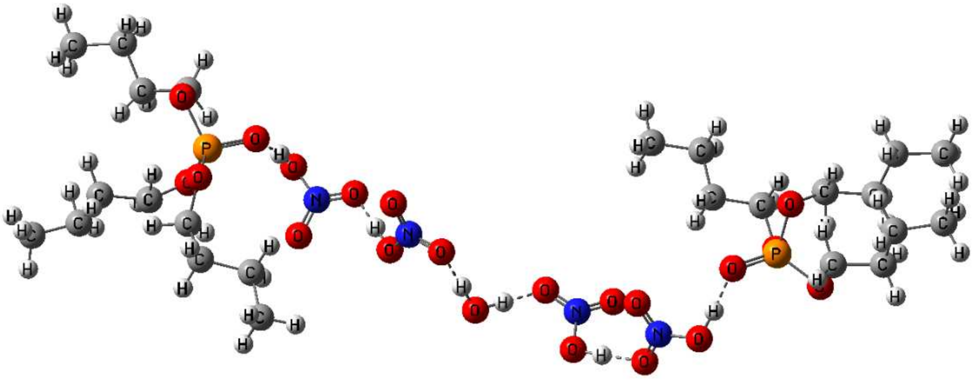

Fig. 5. Suggested structure of the third phase TBP·$2HNO_3$ hemi-solvates

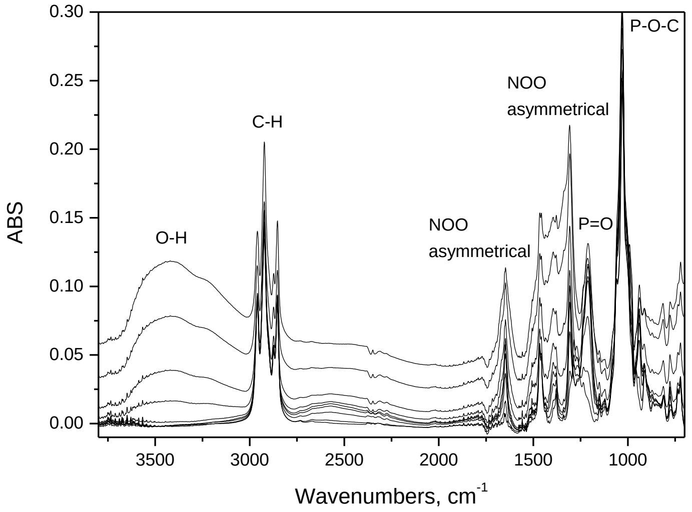

Figure 6. IR spectra of organic phase samples with initial aqueous HNO_3 concentration of 2, 4, 6, 8, 10, 12 and 14 M (from bottom to top)

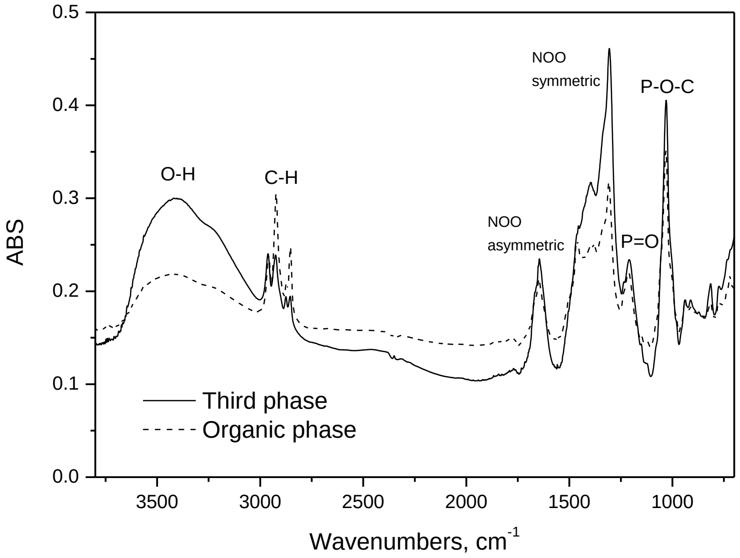

Figure 7. IR spectra of organic vs. third phase samples with initial aqueous HNO_3 concentration of 15.1 M

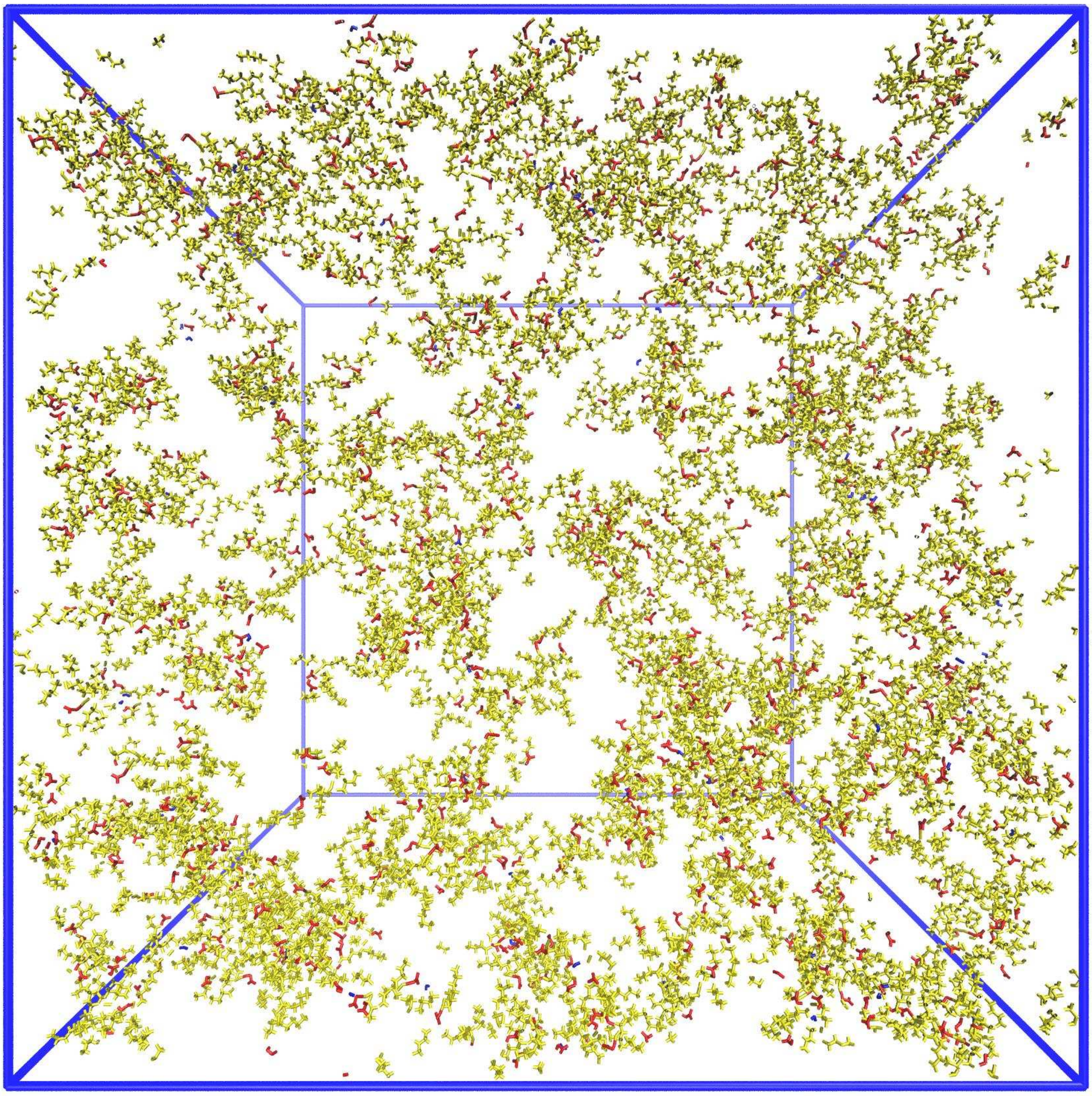

Figure 8. The snapshot of the organic phase system. TBP, HNO_3 and H_2O molecules are represented in yellow, red and blue, respectively; n-dodecane molecules are not shown for clarity

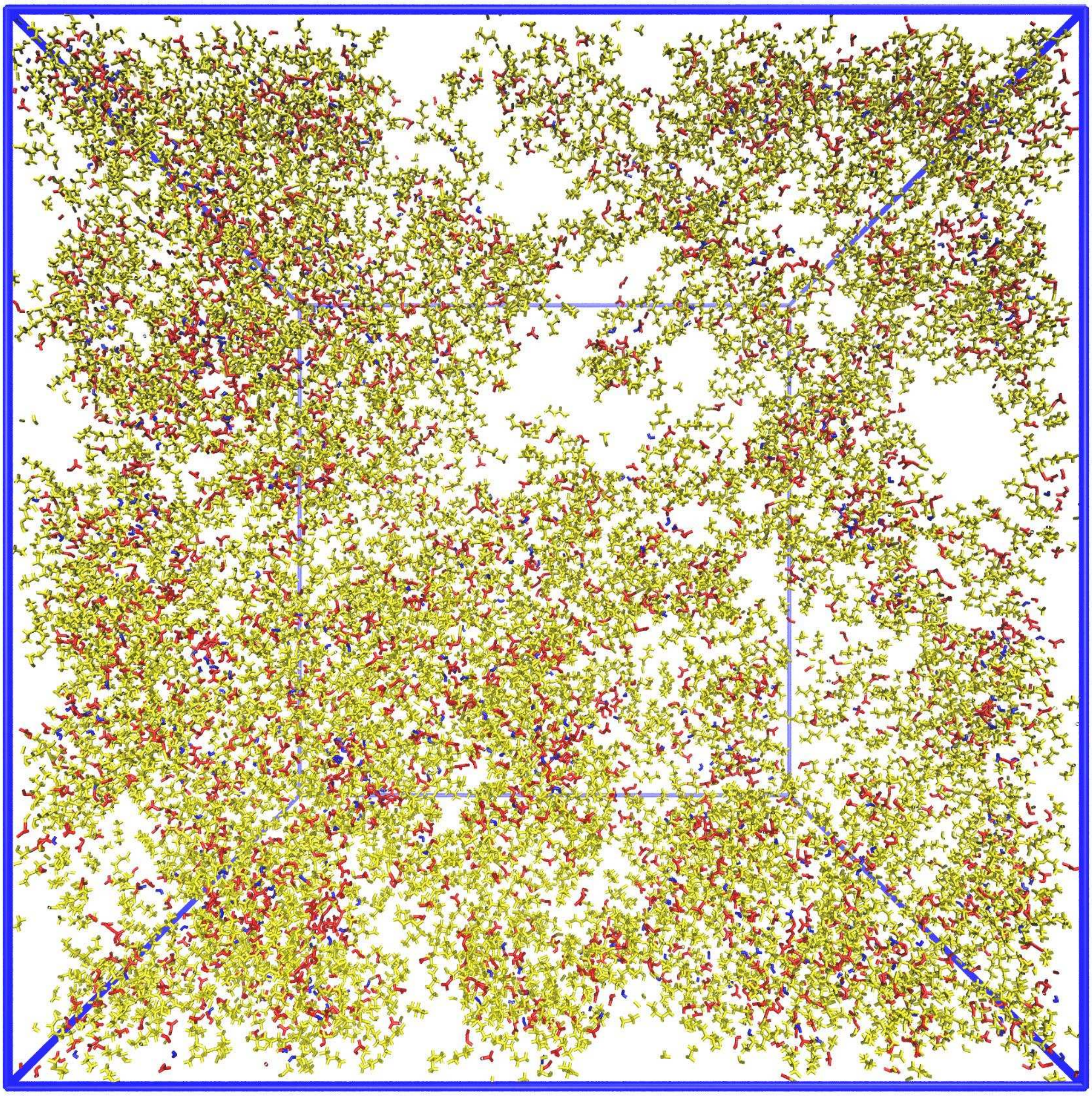

Figure 9. The snapshot of the third phase system. TBP, HNO_3 and H_2O molecules are represented in yellow, red and blue, respectively; n-dodecane molecules are not shown for clarity